Frontiers in Bioscience Landmark

Front. Biosci. (Landmark Ed) **2026**; 31(6): 50834
https://doi.org/10.31083/FBL50834

Original Research

Transcriptomic Insights Into Brassinolide-Mediated Control of Bioactive Compound Biosynthesis in *Salvia miltiorrhiza* Bunge

Wenjiao Ma[1,2,†], Qing Li[3,†], Wenhui Wu[1], Cuicui Han[1,2], Ruibing Chen[2], Xiaoyun Sun[1,2], Yonghao Duan[4], Luyao Yu[2], Zheng Zhou[2,*], Ying He[2,*]

[1]College of Food Science and Technology, Shanghai Ocean University, 201306 Shanghai, China
[2]Navy Special Medical Centre, Naval Medical University, 200433 Shanghai, China
[3]Department of Pharmacy, Second Affiliated Hospital of Naval Medical University, 200003 Shanghai, China
[4]The SATCM Key Laboratory for New Resources & Quality Evaluation of Chinese Medicine, Shanghai University of Traditional Chinese Medicine, 201203 Shanghai, China
*Correspondence: zhouzheng@smmu.edu.cn (Zheng Zhou); yinghe@smmu.edu.cn (Ying He)
[†]These authors contributed equally.
Academic Editor: Jen-Tsung Chen
Submitted: 8 February 2026 Revised: 24 April 2026 Accepted: 15 May 2026 Published: 29 June 2026

Abstract

Background: Brassinolide (BR) plays a pivotal role in regulating plant secondary metabolism and can promote the accumulation of bioactive compounds. However, relatively few studies have explored the application of BR in *Salvia miltiorrhiza*, and the mechanistic basis for its function in this context remains poorly understood. **Methods**: In this study, *S. miltiorrhiza* hairy roots were treated with BR at 1 μM and 5 μM. The treated samples were analyzed via high-performance liquid chromatography (HPLC)-based chemical quantification, transcriptomic sequencing, and quantitative real-time polymerase chain reaction (qRT-PCR) validation to systematically elucidate the concentration-dependent and time-dependent molecular mechanisms underlying BR-mediated biosynthesis of tanshinones and salvianolic acids in *S. miltiorrhiza*. **Results**: BR treatment at the 1 μM dose level significantly induced the accumulation of rosmarinic acid, salvianolic acid B, and tanshinone IIA, with respective 1.43, 1.82, and 1.78-fold increases in the levels of these compounds compared to controls. Expression of most key biosynthetic genes involved in the salvianolic acid and tanshinone biosynthesis pathways peaked at 1 h after treatment with 1 μM BR. Further transcriptomic analysis identified 15 significantly upregulated transcription factors that may regulate tanshinone and salvianolic acid biosynthesis. These differentially expressed genes were primarily enriched in the phenylpropanoid and terpenoid pathways. qRT-PCR validation confirmed the consistency and reliability of these transcriptomic data. **Conclusion**: Collectively, these findings reveal that BR treatment enhances secondary metabolism in *S. miltiorrhiza* by orchestrating changes in the expression of key structural genes and transcription factors, providing a theoretical basis for the breeding of high-quality germplasm resources.

Keywords: *Salvia miltiorrhiza*; brassinolide; secondary metabolism; transcription factors

1. Introduction

Salvia miltiorrhiza Bunge, a plant belonging to the genus Salvia in the Lamiaceae family, is an important medicinal herb within the pharmacopoeia of traditional Chinese medicine. Renowned for its ability to promote blood circulation, alleviate stasis, regulate menstruation, and relieve pain, it is widely used in the clinical prevention and treatment of cardiovascular and cerebrovascular diseases, pulmonary fibrosis, and diabetic complications [1,2,3,4]. The medicinal value of *S. miltiorrhiza* is primarily attributed to two major classes of bioactive secondary metabolites: lipophilic diterpenoid quinones (tanshinones) and water-soluble phenolic acids (salvianolic). The tanshinones include tanshinone IIA (Tan IIA), cryptotanshinone (CT) and tanshinone I (Tan I). Among the salvianolic acids, salvianolic acid B (SAB) is the most abundant and exhibits the most prominent activity [2,5]. Recent pharmacological studies have confirmed that tanshinones exert multiple pharmacological effects, including anti-inflammatory, antioxidant, antimicrobial, anti-tumor, and cardiomyocyte-protective activity [6]. Of these metabolites, Tan IIA is the main bioactive compound present within injectable formulations of *S. miltiorrhiza*. Salvianolic acids have additionally attracted significant attention owing to their potent antioxidant, anti-fibrotic, antiplatelet, and neuroprotective properties [7,8]. The synergistic effects of these two classes of compounds constitute the material basis for the efficacy of *S. miltiorrhiza* in preventing and treating cardiovascular and cerebrovascular diseases.

Despite these promising pharmacological properties, the quality of *S. miltiorrhiza* exhibits significant heterogeneity. Owing to multiple factors including geographical origin, cultivation conditions, harvest age, and processing methods, there is considerable fluctuation in the levels of bioactive compounds within *S. miltiorrhiza* preparations, severely hindering the standardization and modernization

of traditional Chinese medicine products [9,10]. The conventional field cultivation model requires a long growing cycle (typically 2–3 years) and remains susceptible to pests, diseases, and continuous cropping obstacles, contributing to yield instability and variable quality. The utilization of *S. miltiorrhiza* hairy root cultures offers a promising alternative approach to producing uniform, high-quality bioactive compounds [11,12]. Hairy roots, induced by *Agrobacterium rhizogenes*, offer advantages such as rapid growth, genetic stability, hormone independence, and the ability to synthesize secondary metabolites similar to the parent plant. These characteristics make them an ideal experimental model for studying the biosynthesis and regulation of bioactive compounds in *S. miltiorrhiza*. Enhancing the metabolic flux of these high-value metabolic pathways in hairy roots through effective elicitation strategies (*e.g.*, exogenous hormones, abiotic stress, and co-culture) has thus emerged as a central focus of research in this field [12].

The biosynthesis of plant secondary metabolites does not occur in isolation but is intricately linked to the plant's overall growth, development, and environmental response networks [13]. Within this network, phytohormones serve as crucial endogenous signaling molecules, acting as core metabolic "switches" and "tuners". Through complex signal transduction cascades, they regulate the activity of specific transcription factors (TFs), thereby directly or indirectly activating or inhibiting the expression of genes encoding key enzymes involved in secondary metabolic pathways, ultimately influencing the accumulation of target products. In *S. miltiorrhiza*, the roles that classical phytohormones play in regulating tanshinone and salvianolic acid synthesis have been thoroughly investigated. Jasmonic acid (JA) and its derivatives (*e.g.*, methyl jasmonate, MeJA) are recognized as one of the most potent elicitors capable of inducing plant defense responses and secondary metabolism [14,15]. Many studies have demonstrated that the exogenous application of JA/MeJA can significantly upregulate the expression of key genes involved in the tanshinone biosynthesis pathway (*e.g.*, *SmDXS*, *SmDXR*, *SmHMGR*, *SmGGPPS*, *SmCPS*, *SmKSL*) and the salvianolic acid pathway (*e.g.*, *SmPAL*, *SmC4H*, *Sm4CL*, *SmTAT*, *SmHPPR*) in *S. miltiorrhiza* hairy roots. This upregulation effectively promotes the simultaneous accumulation of these two classes of bioactive compounds [15,16,17]. This regulatory relationship is primarily mediated by the interaction between the JA signaling pathway and specific TFs (*e.g.*, MYB, bHLH, and AP2/ERF family members). Abscisic acid (ABA) is a primary abiotic stress response hormone that can also effectively induce the synthesis of bioactive compounds in *S. miltiorrhiza* under conditions of simulated drought, salinity, and other forms of stress. ABA treatment can activate specific TFs (*e.g.*, bZIP) involved in tanshinone biosynthesis [10,18], thereby driving the expression of downstream structural genes and promoting tanshinone accumulation. Concurrently, extensive crosstalk exists between the ABA and JA signaling pathways, enabling precise metabolic reprogramming under stress. Unlike the inducing effects of JA and ABA, gibberellic acid (GA) primarily promotes plant cell elongation and division [19]. Interestingly, some research suggests that GA signaling may play a negative regulatory role in tanshinone synthesis [20,21]. When the core inhibitory factors of the GA signaling pathway, DELLA proteins (*e.g.*, RGA), are suppressed, their inhibition of positive regulatory TFs (*e.g.*, MYC2) involved in salvianolic acid synthesis is disrupted, thereby indirectly promoting the synthesis of this metabolite under specific conditions [21]. This underscores the importance of phytohormone balance in the regulation of metabolic flux. In summary, phytohormones comprise a complex and precise regulatory network governing the synthesis of bioactive compounds in *S. miltiorrhiza*. A comprehensive understanding of these phytohormone-mediated regulatory mechanisms therefore provides the theoretical foundation necessary to develop efficient metabolic engineering strategies.

Brassinosteroids (BRs) are a class of polyhydroxylated sterol phytohormones that include multiple compounds, such as BR, 24-epibrassinolide (24-EBL), and 28-homobrassinolide (28-HBL), with naturally occurring BR being the most bioactive member of this family [22,23]. Since their discovery in the 1970s, BRs have been established as indispensable global regulators of plant growth and developmental processes (*e.g.*, cell elongation and division, vascular differentiation, photomorphogenesis, and pollen tube growth) as well as stress adaptation (*e.g.*, resistance to cold, heat, drought, and disease) [24,25]. BRs signal through the cell-surface receptor kinase BRI1, which heterodimerizes with the co-receptor BAK1 and initiates a phosphorylation cascade, ultimately activating the downstream TFs BZR1/BZR2 to regulate the expression of genes involved in growth, development, and secondary metabolism [26]. Increasing evidence indicates that BRs also play a key role in regulating plant secondary metabolism. For instance, in *Arabidopsis*, BRs signaling regulates the flavonoid biosynthesis pathway through TFs BES1/BZR1; in tomatoes, BRs promote the accumulation of polyphenols and carotenoids; in medicinal plants (*e.g.*, *Panax ginseng*, *Catharanthus roseus*, and *Astragalus membranaceus*), exogenous treatment with BRs has been shown to significantly increase the content of specific bioactive compounds (*e.g.*, saponins, alkaloids, and flavonoids) [24,27,28]. The biological functions of BRs are mediated through a highly conserved signal transduction pathway wherein BRs are recognized by the cell surface receptor kinase BRI1, triggering a series of phosphorylation cascades that ultimately lead to the accumulation and nuclear translocation of the core transcription factors BZR1 and BES1 [29,30,31]. Within the nucleus, these TFs directly bind to BR response elements (BRRE/E-box) on target gene promoters or interact with other TFs, leading to the

large-scale reprogramming of the gene expression network. This demonstrates that BRs have the significant potential to directly regulate rate-limiting enzyme genes and key TFs involved in secondary metabolic pathways [25]. However, in stark contrast to the in-depth research conducted to date on phytohormones such as JA and ABA, systematic studies exploring how BRs affect the synthesis of bioactive compounds in the important medicinal model plant *S. miltiorrhiza* are still lacking.

In the present study, BR, as the most bioactive member of the BR family, was selected as the research subject to systematically investigate the regulatory effects and underlying mechanisms through which exogenous BR influences the growth of *S. miltiorrhiza* hairy roots and the biosynthesis of the core bioactive compounds, tanshinones and salvianolic acids. Based on preliminary experimental results, hairy roots were treated with a series of BR concentration gradients (*e.g.*, 1 μM, 5 μM, and 10 μM). Two representative concentrations (1 μM and 5 μM) were selected for use in this study, as they have previously been reported to exert significant positive regulatory effects on plant secondary metabolism. Higher concentrations may exert contrasting effects, including the suppression of root development and the induction of physiological and metabolic disorders [32,33,34]. Samples were taken at different time points post-treatment to capture dynamic responses. Quantification of bioactive compound contents confirmed the regulatory effect of BR treatment in promoting bioactive compound accumulation in *S. miltiorrhiza*. At key time points after BR treatment, high-throughput transcriptome sequencing was performed on control and treated hairy roots (1 μM and 5 μM BR). Bioinformatics analysis was employed to identify differentially expressed genes (DEGs) induced or suppressed by BR treatment. Through Kyoto Encyclopedia of Genes and Genomes (KEGG) and Gene Ontology (GO) enrichment analyses, the major biological processes and metabolic pathways influenced by BR exposure were identified. The expression patterns of all key structural genes involved in the tanshinone and salvianolic acid synthesis pathways were precisely mapped. Subsequently, key TFs potentially subject to direct BR-mediated regulation were screened and analysed. Taken together, the results offer novel insights into the mechanisms by which steroidal hormones regulate secondary metabolism in *S. miltiorrhiza,* while also establishing a solid theoretical and experimental foundation for the use of BR or downstream signaling pathway components as targets for metabolic engineering efforts aimed at cultivating high-content *S. miltiorrhiza* germplasm resources or optimizing associated hairy root cultivation in an industrial setting.

2. Materials and Methods

2.1 Plant Materials and Treatments

S. miltiorrhiza hairy roots were used as the experimental material. Sterile plantlets (1-month-old) were subjected to Agrobacterium-mediated transformation using the leaf disc method to induce hairy root formation. *Agrobacterium rhizogenes* strain C58C1 harboring the empty vector pCAMBIA1300 was used to infect leaf explants excised from sterile *S. miltiorrhiza* seedlings. Following co-cultivation for 2–3 days, the explants were transferred to a selection medium supplemented with an appropriate antibiotic (*e.g.*, cefotaxime sodium) to eliminate *Agrobacterium* and induce hairy root formation. After approximately 2–3 weeks, hairy roots emerging from the cut edges of the explants were excised and subcultured to establish independent lines, thereby generating empty vector-transformed control hairy root materials for subsequent experiments. The leaf explants were derived from axenic seedlings grown *in vitro* from seeds acquired from the Chinese Academy of Agricultural Sciences. The resulting hairy roots were cultured in darkness at 25 °C. For experimental use, the hairy roots were cultured in Murashige and Skoog basal medium (M519; PhytoTechnology Laboratories, Lenexa, KS, USA) containing 3% sucrose, 0.8% agar, 150 mg/L cefotaxime sodium (J1109-2; Yuanmeng Biotech, Hubei, China), and adjusted to a pH of 5.8. The cultures were maintained at 25 °C on a shaker at 150 rpm. On day 25 of culture, the hairy roots were treated with exogenous BR at a final concentration of 1 μM or 5 μM. Five biological replicates were established for each treatment group. Samples were collected at 0 h, 1 h, and 3 h post-treatment, immediately frozen in liquid nitrogen, and stored at –80 °C until further use.

2.2 Analysis of Bioactive Compounds

Hairy root samples were dried to constant weight in an oven, ground into a fine powder, and passed through a 200-mesh sieve. Exactly 0.015 g of the powder was weighed into a 50 mL stoppered Erlenmeyer flask, and 5 mL of 80% methanol was added. The mixture was ultrasonicated at 500 W and 45 kHz for 30 min (Ningbo Scientz Biotechnology Co., Ltd., Ningbo, China), equilibrated to room temperature, and then centrifuged at 8000 rpm for 10 min. The supernatant was filtered through a 0.22-μm membrane, and the bioactive compounds therein were quantified by high-performance liquid chromatography (HPLC, Agilent Technologies, Santa Clara, CA, USA) [35]. A Diamonsil® C18(2) column (250 mm × 4.6 mm, 5 μm, Dikma Technologies, Beijing, China) was used for separation. The column temperature was maintained at 23 °C, and the detection wavelength was set at 270 nm. The mobile phase consisted of 0.08% formic acid aqueous solution (phase A) and acetonitrile (phase B) with a gradient elution program as follows: 10%–40% phase B (0–15 min), then increased to 76% phase B at 30 min, followed by an isocratic elution with 76% phase B for 15 min (30–45 min). The flow rate was fixed at 1.0 mL/min, and the injection volume was 10 μL [36].

The following reference substances were used: danshensu (DSS, ≥98%, B20536; Shanghai Yuanye

Bio-Technology Co., Ltd., Shanghai, China), 4-hydroxyphenyllactic acid (4-HPL, ≥98%, B29875; China), caffeic acid (CA, ≥98%, B20512; China), rosmarinic acid (RA, ≥98%, B20550; China), salvianolic acid A (SAA, ≥98%, B20541; China), SAB (≥98%, B20540; China), CT (≥98%, B20545; China), Tan I (≥98%, B20546; China), and Tan IIA (≥98%, B20547; China). Each reference substance was transferred into a 10 mL volumetric flask, dissolved in methanol, and brought to volume to prepare individual standard stock solutions. Subsequently, 1.0 mL of each individual standard stock solution was accurately measured, mixed, and then diluted 10-fold with methanol to prepare a mixed reference stock solution. The resulting solution was stored at 4 °C for subsequent use.

2.3 RNA-Sequencing (RNA-Seq) Libraries Construction and Sequencing

Total RNA was extracted from samples using a TransZol UP Plus RNA Kit (ER501; TransGen Biotech Co., Ltd., Beijing, China). RNA quality was evaluated with an Agilent 2200 system (Agilent Technologies, Santa Clara, CA, USA), and RNA samples with an RNA integrity number (RIN) >7.0 were used for cDNA library construction. The cDNA libraries were constructed for each RNA sample using the VAHTS Universal V6 RNA-seq Library Prep Kit for Illumina (NR604; Nanjing Vazyme Biotech Co., Ltd., Nanjing, China) according to the manufacturer's instructions. Generally, the protocol consisted of the following steps: Poly(A)-containing mRNA was purified from 1 μg of total RNA using oligo(dT) magnetic beads and fragmented into 200–600 bp fragments using divalent cations at 85 °C for 6 minutes. The cleaved RNA fragments were used for first- and second-strand cDNA synthesis. A dUTP mix was used for second-strand cDNA synthesis, allowing for the removal of the second strand. The cDNA fragments were then subjected to end repair, A-tailing, and indexed adapter ligation. The ligated cDNA products were purified and treated with uracil DNA glycosylase to remove the second-strand cDNA. Purified first-strand cDNA was then enriched by PCR to establish the cDNA libraries. These libraries underwent quality control with an Agilent 2200 instrument, followed by 150 bp paired-end sequencing on a DNBSEQ-T7 instrument.

2.4 RNA-Seq Data Cleaning and Alignment

To ensure the accuracy of subsequent analyses, raw reads from sequencing were filtered and purified to obtain high-quality clean reads. Reads containing adapter sequences, low-quality bases (Q-value <20 bases with >50%), and unknown bases were removed. The number of clean reads per sample, proportions of bases with Q20 and Q30, and GC content were then calculated.

Clean reads were then aligned to the *S. miltiorrhiza* genome (NGDC accession number: PRJCA003150) using the Hisat2 [37]. HTseq [38] was used to obtain gene counts, while gene expression was determined using the FPKM method.

2.5 Quantification of Gene Expression Levels and Differential Expression Analysis

We applied the EBSeq algorithm [39] to filter out DEGs, while gene expression was determined using the $|\log_2 FC| \geq 1$ and q-value ≤ 0.05 [40].

2.5.1 Transcription Factor Database Annotation

The HMMER 3.3.2 software (Howard Hughes Medical Institute, Janelia Research Campus, Ashburn, VA, USA) was used for domain scanning of Unigene sequences, referencing to the conserved domains for each TF family obtained from the PlantTFDB v5.0 database (https://planttfdb.gao-lab.org/prediction.php). After cross-referencing the BLASTp alignment results and PlantTFDB (identity ≥50%, coverage ≥70%), redundant sequences were eliminated to determine the candidate TF sequences and their family classifications.

2.5.2 GO Analysis

GO analysis was performed to explore the potential biological implications of the identified DEGs [41]. GO annotations were downloaded from the NCBI (http://www.ncbi.nlm.nih.gov/), UniProt (http://www.uniprot.org/), and Gene Ontology (http://www.geneontology.org/) databases. Fisher's exact test was used to identify significant GO term enrichment (q-value ≤ 0.05).

2.5.3 KEGG Pathway Analysis

Significant KEGG pathway enrichment for the identified DEGs was identified through the KEGG database using Fisher's exact test, with q-value ≤ 0.05 as the significance threshold [42].

2.5.4 Quantitative Real-Time PCR (qRT-PCR) Validation

Total RNA was extracted from the hairy root samples using TransZol UP Plus RNA Kit. The RNA concentration and purity were determined by NanoDrop 2000 spectrophotometry (Thermo Fisher Scientific, Waltham, MA, USA). For qRT-PCR analysis, approximately 500 ng of total RNA from each sample was used as a template. The reactions were performed using the TransScript®Green One-Step qRT-PCR SuperMix (AQ211-01; TransGen Biotech, Beijing, China) on a LightCycler®96 real-time PCR system (Roche Diagnostics, Mannheim, Germany), with Sm18S as the internal control. The thermal cycling protocol was as follows: 45 °C for 5 min, 94 °C for 30 sec, followed by 45 cycles of 94 °C for 5 sec and 60 °C for 30 sec. The experiments were conducted three times. The relative expression levels of selected genes were calculated using the $2^{-\Delta\Delta Ct}$ method. The primer sequences used in this study are listed in **Supplementary Table 1**.

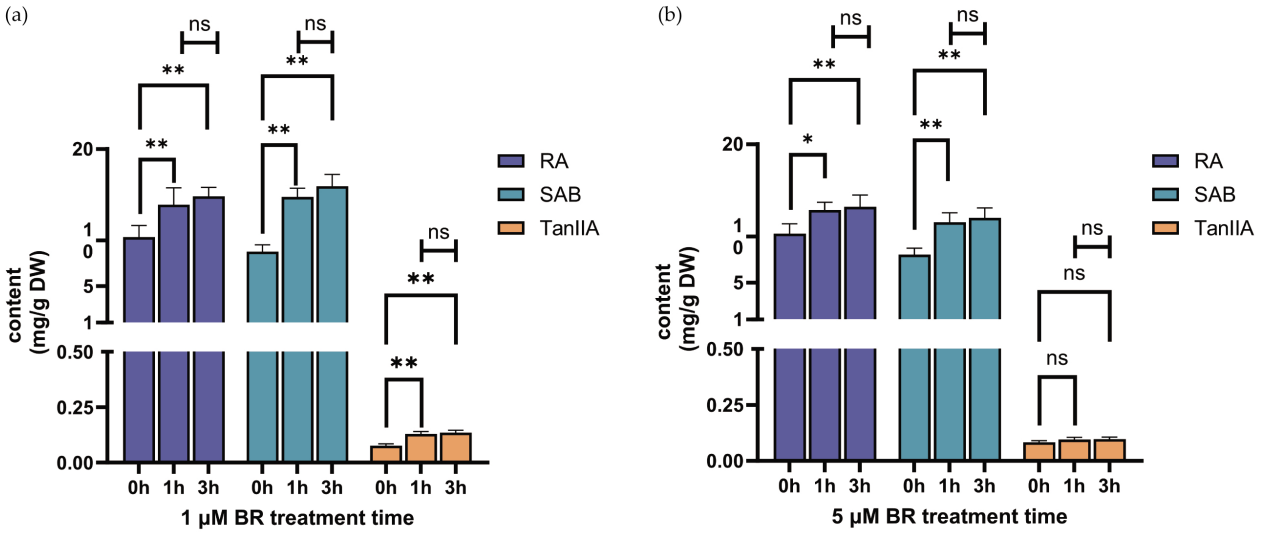

Fig. 1. RA, SAB and Tan IIA content in BR-treated hairy roots over time. (a) RA, SAB, and Tan IIA content at 0, 1, and 3 h under 1 μM BR. (b) RA, SAB, and Tan IIA content at 0, 1, and 3 h under 5 μM BR. BR, brassinolide; RA, rosmarinic acid (blue); SAB, salvianolic acid B (green); Tan IIA, tanshinone IIA (orange). Error bars indicate the standard deviation (SD) (n = 5 biological replicates). Statistical significance was determined by Student's *t*-test. Asterisks denote statistically significant differences with 0 h: $*p < 0.05$; $**p < 0.01$; ns, not significant.

3. Results

3.1 Accumulation of Bioactive Compounds in S. miltiorrhiza Under BR Treatment

HPLC was employed to quantify the levels of RA, SAB and Tan IIA in *S. miltiorrhiza* hairy roots harvested at different time points under 1 μM and 5 μM BR treatments (Fig. 1). Compared with the control group (0 h), treatment with 1 μM BR for 1 h significantly increased the contents of all three compounds, and these levels remained stable at 3 h. Specifically, after 1 h of 1 μM BR treatment, the levels of RA, SAB, and Tan IIA increased to 1.34-fold, 1.68-fold, and 1.70-fold relative to the control, respectively; at 3 h, they reached 1.43-fold, 1.82-fold, and 1.78-fold, respectively, with no significant difference between the 1 h and 3 h time points. Following 5 μM BR treatment, the levels of phenolic acids (RA and SAB) were significantly elevated compared to the control, with corresponding increases of 1.25-fold and 1.44-fold at 1 h, and 1.28-fold and 1.50-fold at 3 h, respectively. In contrast, Tan IIA levels did not differ significantly at any time point under 5 μM BR treatment. Furthermore, no significant differences were observed between the 1 h and 3 h time points for any compound under 5 μM BR treatment. Notably, at the same time points, the increases induced by 5 μM BR treatment were consistently lower than those observed with 1 μM BR treatment. These results demonstrate that low-concentration BR exposure promotes the accumulation of bioactive metabolites in a time-dependent manner, whereas the stimulatory effect of high-concentration BR is more limited.

3.2 Transcriptomic Sequencing

To further investigate the regulatory mechanisms underlying the accumulation of tanshinones and salvianolic acids in *S. miltiorrhiza*, transcriptome sequencing was performed on hairy roots treated with both tested BR concentrations (1 μM, 5 μM) at 0 h, 1 h, and 3 h time points. The total number of raw reads across the 30 samples ranged from 38.96 to 53.37 million, corresponding to 5.84 to 8.01 gigabases of raw base pairs. After filtering, the number of high-quality clean reads per sample ranged from 38.96 to 53.37 million, corresponding to 5.80 to 7.94 gigabases of clean bases. The proportion of clean bases relative to raw bases was at least 99.04%. The proportion of bases with a Phred quality score of Q20 (≥99% accuracy) exceeded 98.88%, and the Q30 proportion (≥99.9% accuracy) was ≥95.31% (**Supplementary Table 2**).

As presented in **Supplementary Table 3**, the mapping rate of clean reads to the reference genome ranged from 93.39% to 95.38%, indicating the successful alignment of most sequences. The ratio of multiple mapped reads ranged from 7.24% to 16.11%, whereas the uniquely mapped read ratio was ≥79.27%. Overall, these results demonstrate that the sequencing data are of high quality and suitable for subsequent bioinformatics analysis.

3.3 Analysis of DEGs Under BR Treatment

To characterize the transcriptional dynamics elicited by BR treatment in *S. miltiorrhiza* hairy roots, we performed RNA-Seq analysis, and these transcriptomic data were subjected to further analysis. For the 1 μM BR dose level, 1 h of exposure resulted in 6594 DEGs (3560 upreg-

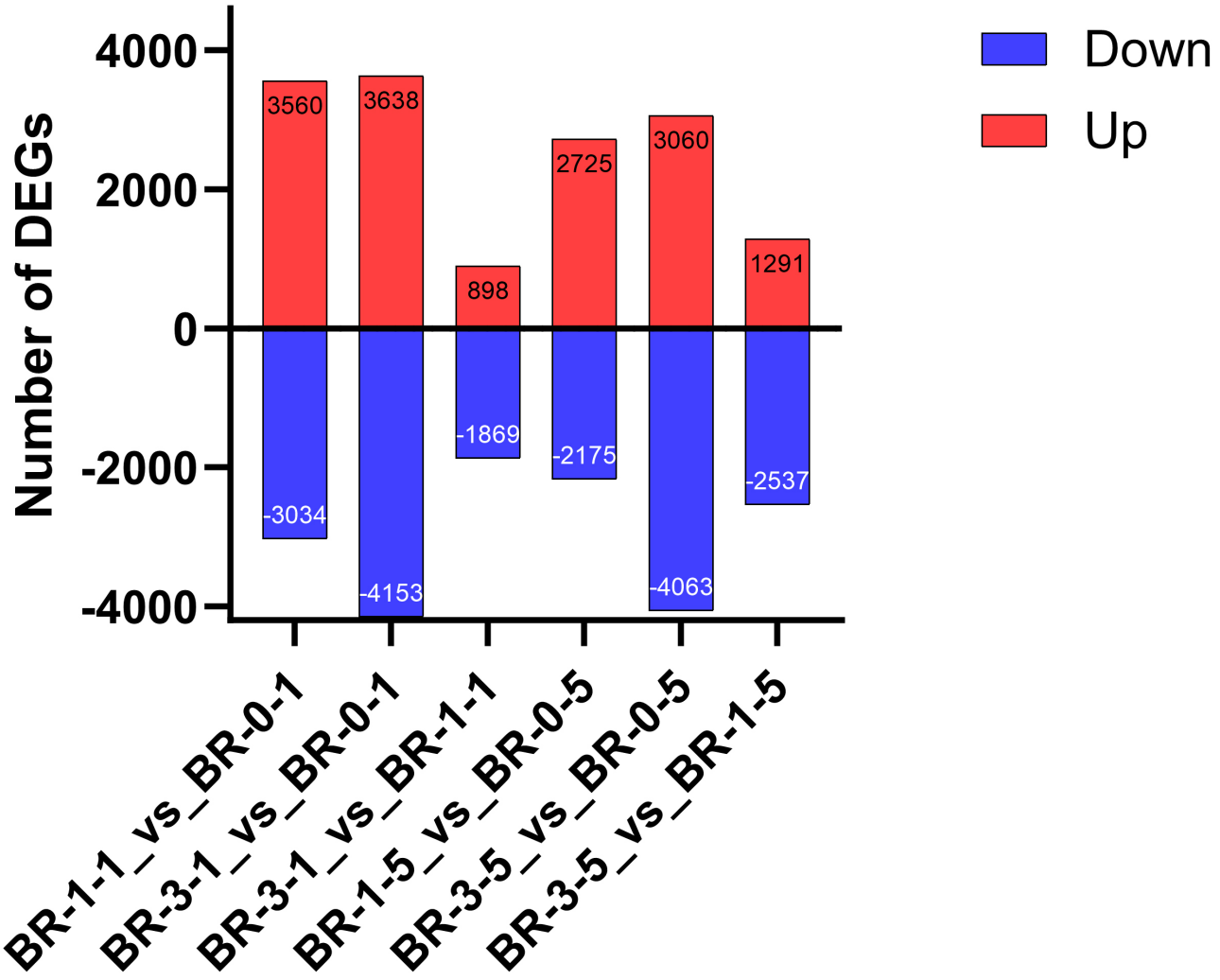

Fig. 2. DEG quantification in *S. miltiorrhiza* hairy roots subjected to BR treatment. The expression profiles of samples treated with 1 μM BR for 1 h (BR-1-1) and 3 h (BR-3-1) were compared to the control group (BR-0-1), as well as between the two treatment groups. The same comparisons were made for samples treated with 5 μM BR for 1 h (BR-1-5) and 3 h (BR-3-5) relative to the control (BR-0-5), and between the two 5 μM treatment groups. "Up" and "Down" indicate significant up-regulation (red) and down-regulation (blue) of gene expression, respectively, compared with the indicated reference group. Differentially expressed genes were defined using thresholds of $|\log_2 FC| \geq 1$ and q-value ≤ 0.05.

ulated and 3034 downregulated), while the total number of DEGs after 3 h rose to 7791 (3638 upregulated and 4153 downregulated). Direct comparison between the 3 h and 1 h time points at this concentration revealed 2767 DEGs (898 upregulated and 1869 downregulated). At the higher BR dose level (5 μM), 4900 DEGs were detected at 1 h (2725 upregulated and 2175 downregulated), whereas 7123 DEGs (3060 upregulated and 4063 downregulated) were observed at 3 h. Comparison of the 3 h and 1 h time points for 5 μM BR treatment yielded 3828 DEGs, including 1291 upregulated and 2537 downregulated genes. Regardless of the BR concentration employed, the total number of DEGs reached its highest level at 3 h, at which time the number of downregulated genes also peaked and exceeded that of upregulated genes. The increase in the number of upregulated genes from 1 h to 3 h was less pronounced than that of downregulated genes. The total number of DEGs was higher in the 1 μM BR treatment group compared to the 5 μM group (Fig. 2).

3.4 Expression Patterns of Key Genes Involved in Tanshinone and Salvianolic Acids Biosynthesis in S. miltiorrhiza

To investigate the regulatory effects of BR on the biosynthesis of major bioactive compounds in *S. miltiorrhiza*, heatmap analysis was performed to examine the expression patterns of genes encoding key enzymes in the salvianolic acid and tanshinone biosynthetic pathways over time and at different BR treatment levels. As shown in Fig. 3a, most genes in the salvianolic acid biosynthetic

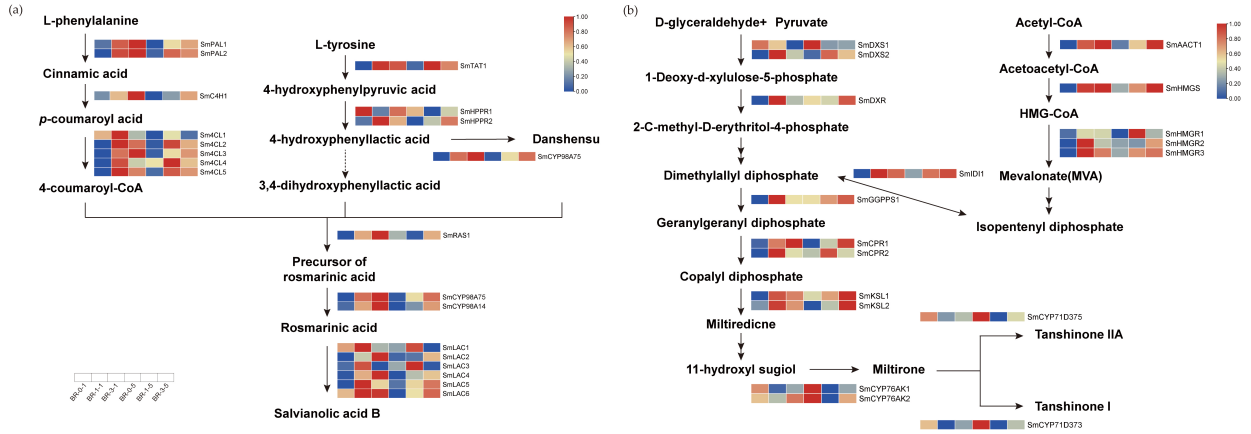

Fig. 3. Expression profiles of individual selected genes involved in tanshinone and salvianolic acid biosynthesis under BR stimulation. (a) Expression of genes encoding key enzymes involved in the salvianolic acid biosynthetic pathway. (b) Expression of genes encoding key enzymes involved in the tanshinone biosynthetic pathway. Heatmaps were generated using $\log_2$-transformed FPKM values with row Z-score normalization. A deeper red color indicates a higher expression level, while deeper blue colors denote lower expression.

pathway, including *SmPAL1*, *SmC4H1*, *Sm4CL1*, *SmTAT1*, *SmRAS1*, and *SmCYP98A14*, were markedly induced after BR treatment. Under BR treatment, the expression levels of most genes peaked at 1 h, followed by a slight decrease at 3 h, while remaining upregulated compared to the control (0 h). With respect to the tanshinone biosynthesis pathway, key genes such as *SmDXS*, *SmGGPPS*, *SmCPS*, *SmKSL*, *SmAACT*, *SmHMGR*, and *SmHMGS* were also remarkably induced by BR treatment (Fig. 3b). Under 1 μM BR treatment, the expression of most tanshinone pathway genes peaked at 1 h and slightly declined at 3 h. In contrast, under 5 μM BR treatment, the expression of most genes gradually increased with time. Overall, the extent of induction for these biosynthetic genes was greater under low-concentration BR treatment, especially at early time points.

3.5 Functional Enrichment Analysis of DEGs

To elucidate the functional characteristics of these DEGs, GO functional enrichment analysis was performed. For the BR-1-1 vs. BR-0-1 comparison, the most enriched biological process (BP) category was Response to Stimulus, while the most enriched cellular component (CC) categories were Plasma Membrane and Cell Periphery, and the most enriched molecular function (MF) category was Catalytic Activity (Fig. 4a). Compared with the control group, DEGs in the BR-3-1 group were most significantly enriched in the Response to Stimulus (BP), Plasma Membrane (CC), and Catalytic Activity (MF) categories (Fig. 4b). The DEGs identified from the BR-1-5 vs. BR-0-5 were enriched in Response to Stimulus and Response to Chemical (BP), Plasma Membrane (CC), and Catalytic Activity (MF) categories (Fig. 4c). For the BR-3-5 vs. BR-0-5 comparison, the identified DEGs were most enriched in the Response to Stimulus and Response to Chemical (BP), Plasma Membrane (CC), as well as Catalytic Activity and Oxidoreductase Activity (MF) categories (Fig. 4d).

To further investigate the metabolic pathways associated with these changes in gene expression, KEGG pathway enrichment analysis was performed on the differentially expressed genes. A total of 173, 182, 181, and 194 KEGG pathways were identified for the BR-1-1 vs. BR-0-1, BR-3-1 vs. BR-0-1, BR-1-5 vs. BR-0-5, and BR-3-5 vs. BR-0-5 comparisons, respectively. Using a q-value ≤ 0.05 as the threshold, the top 10 significantly enriched metabolic pathways were selected for each of the four treatment groups. DEGs for the BR-1-1 vs. BR-0-1 comparison were primarily enriched in pathways related to carbohydrate metabolism, signal transduction, amino acid metabolism, and phenylpropanoid biosynthesis. For the BR-3-1 vs. BR-0-1 comparison, carbohydrate metabolism, signal transduction, phenylpropanoid biosynthesis, and metabolism of terpenoids and polyketides were among the top-enriched categories. In the BR-1-5 vs. BR-0-5 comparison, carbohydrate metabolism, plant hormone signal transduction, and cytochrome P450 were the most prominent categories. For the BR-3-5 vs. BR-0-5 comparison, the predominant pathways were signal transduction, metabolism of terpenoids and polyketides, and phenylpropanoid biosynthesis. Pathways related to carbohydrate metabolism, signal transduction, terpenoid/polyketide metabolism, phenylpropanoid biosynthesis, and cytochrome P450 were consistently enriched across most comparisons. The complete list of the top 10 enriched pathways for each comparison is presented in the Fig. 4e.

3.6 Identification of TFs Responsive to BR Induction

BR strongly influences the secondary metabolism of *S. miltiorrhiza* by regulating the expression of pathway-related genes, with TFs playing pivotal intermediary roles in this regulatory network. *SmbHLH148* overexpression in *S. miltiorrhiza* increases salvianolic acids and tanshinones

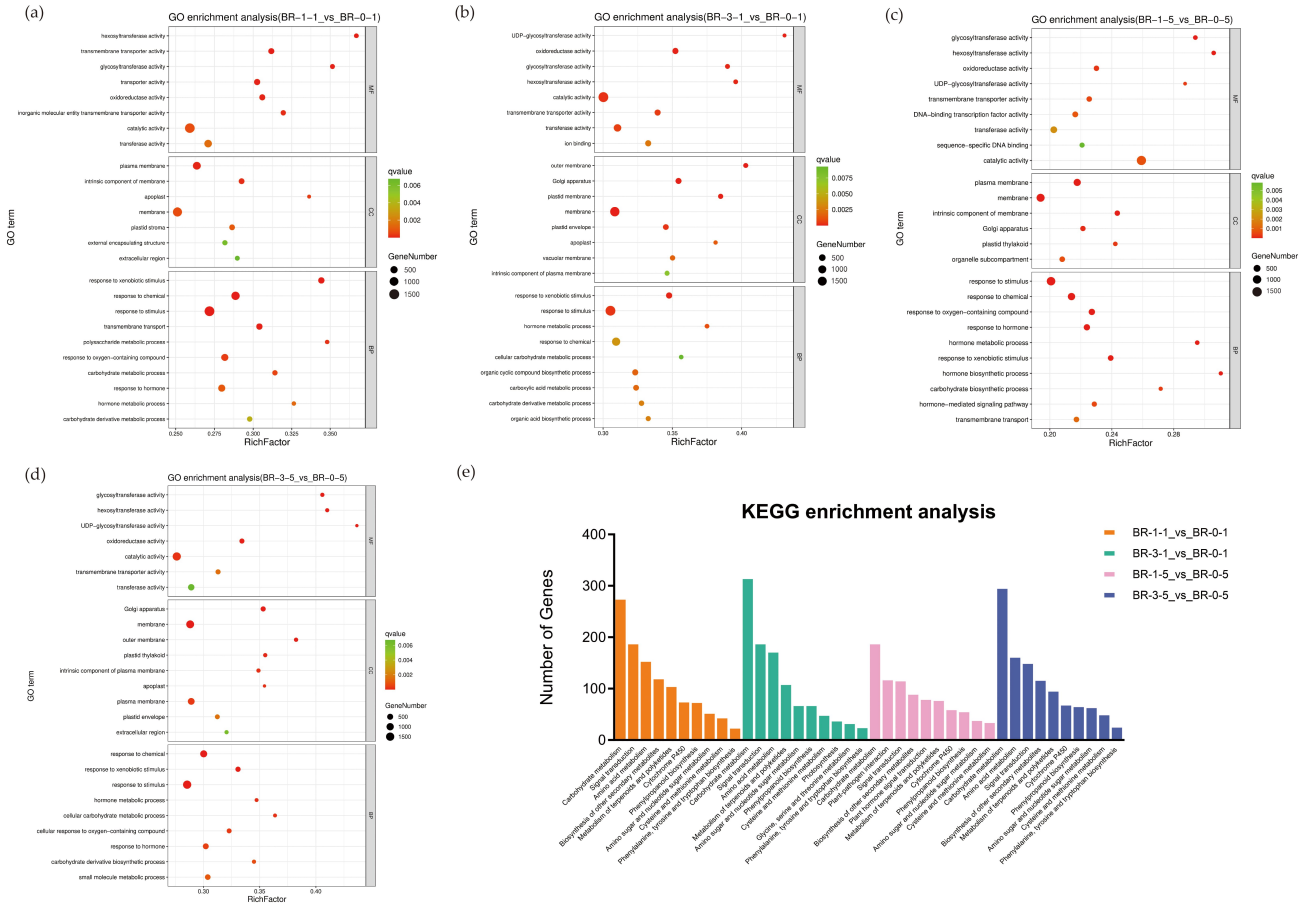

Fig. 4. Functional enrichment analysis of identified DEGs. (a) GO enrichment analysis of DEGs identified for the BR-1-1 vs. BR-0-1 comparison. (b) GO enrichment analysis of DEGs identified for the BR-3-1 vs. BR-0-1. (c) GO enrichment analysis of DEGs identified for the BR-1-5_vs_BR-0-5 comparsion. (d) GO enrichment analysis of DEGs identified for the BR-3-5 vs. BR-0-5 comparison. In (a–d), the ordinate indicates the GO term, and the abscissa indicates the enrichment factor. Bubble size is proportional to the number of genes, while the color scale represents the significance level (q-value), with darker red indicating greater significance. The top enriched terms with the largest number from the MF, BP and CC categories are displayed. (e) KEGG pathway enrichment analysis of DEGs in *S. miltiorrhiza* hairy roots induced by BR. The bar graph shows the enriched pathways for four comparison groups: BR-1-1 vs BR-0-1 (orange), BR-3-1 vs BR-0-1 (green), BR-1-5 vs BR-0-5 (pink), and BR-3-5 vs BR-0-5 (blue).

production (SAB and Tan I increased 5.99-fold and 3.97-fold, respectively) and upregulates biosynthetic genes [43]. Consistently, we observed upregulation of *SmbHLH148* following BR induction. *SmWRKY61* overexpression enhances Tan I and Tan IIA production (11.09-fold and 33.37-fold, respectively) and broadly upregulates tanshinone biosynthetic genes [44]. BR treatment also induced a slight upregulation of *SmWRKY61* in our study. While TFs such as *SmbHLH148* that potentially mediate the BR-regulated biosynthesis of tanshinones and salvianolic acids have been identified, unknown components still exist in this regulatory network. To further elucidate the transcriptional mechanisms by which the BR signaling pathway regulates secondary metabolism in *S. miltiorrhiza*, systematic screening and validation of other key TFs that respond to BR and regulate the biosynthesis of both tanshinones and salvianolic acids are therefore needed.

Using the PlantTFDB v5.0 database, 1736 TFs belonging to 55 families (55 all) were identified from 29,236 protein sequences within the *S. miltiorrhiza* genome (NGDC accession number: PRJCA003150). For the BR-1-1 vs. BR-0-1 comparison group, a total of 438 differentially expressed TFs (DETFs) were detected, including 283 upregulated and 155 downregulated TFs classified into the AP2/ARF, B3, bHLH, bZIP, C2H2, C3H, Dof, ERF, GATA, GRAS, HD-ZIP, LBD, MYB, NAC, TCP, and WRKY families. For the BR-3-1 vs. BR-0-1 comparison, the number of DETFs increased to 442 (192 upregulated and 250 downregulated), and was primarily associated with the AP2, ARF, B3, bHLH, bZIP, C2H2, C3H, Dof, ERF, GRAS, MIKC_MADS, HD-ZIP, LBD, MYB, NAC, and WRKY families. For the BR-1-5 vs. BR-0-5 comparison, 393 DETFs were identified (238 upregulated and 155 downregulated), and they were

predominantly assigned to families including the AP2, bHLH, bZIP, C3H, ERF, GATA, GRAS, MIKC_MADS, HD-ZIP, LBD, MYB, NAC, and WRKY families. For the BR-3-5 vs. BR-0-5 comparison, the number of DETFs rose to 430 (169 upregulated and 261 downregulated), primarily belonging to the AP2, bHLH, bZIP, C2H2, ERF, MIKC_MADS, HD-ZIP, LBD, MYB, NAC, TCP, and WRKY families. Based on the criterion of more than 40 family members being present in this dataset, the top 15 TF families (15 maj) were identified as the MYB, bHLH, AP2/ERF, C2H2, NAC, WRKY, bZIP, GRAS, LBD, G2-like, HD-ZIP, MIKC_MADS, B3, FAR1, and C3H families (Fig. 5a). Across the four treatment groups (BR-1-1, BR-3-1, BR-1-5, BR-3-5), a total of 94 upregulated DETFs (94 sec) were identified (Fig. 5b). These 94 TFs were categorized into 23 families, 12 of which overlapped with the top 15 families identified above, including the bHLH, bZIP, AP2/ERF, MYB, NAC, G2-like, GRAS, HD-ZIP, C3H, C2H2, LBD, and WRKY families. These 12 families contained 19, 5, 13, 9, 4, 1, 2, 2, 4, 3, 5, and 7 co-upregulated DETFs, respectively, accounting for 74 TFs in total (Fig. 5c,d). Given that major bioactive components present in *S. miltiorrhiza* (*e.g.*, Tan IIA and SAB) predominantly accumulate in the roots, the tissue expression profiles for these 70 TFs were analyzed (note: expression profiles of the remaining 4 TFs were unavailable). This screening effort identified 15 candidate TFs that were highly expressed in roots and potentially involved in salvianolic acid and tanshinone biosynthesis: EVM0012259, EVM0023360, EVM0020612, EVM0001404, EVM0005048, EVM0027421, EVM0010408, EVM0024997, EVM0022018, EVM0023863, EVM0006157, EVM0005118, EVM0026250, EVM0002972, and EVM0026210. These TFs exhibited significant upregulation at 1 h post-treatment, with expression levels either sustained at the 1 h level or moderately declined (Fig. 5e).

3.7 qRT-PCR Validation of Selected Biosynthetic Genes and Candidate TFs

To validate the reliability of these RNA-Seq data, qRT-PCR was used to analyze the expression of selected genes involved in the biosynthetic pathways, as well as candidate TFs (Fig. 6). Because the 1 μM BR treatment induced more pronounced expression trends than the 5 μM treatment, we focused our validation on the 1 μM condition. For the salvianolic acid pathway, we selected *SmPAL1*, *Sm4CL3*, *SmRAS1*, *SmCYP98A75*, *SmCYP98A14*, and *SmLAC5*; for the tanshinone pathway, we selected *SmAACT1*, *SmDXS*, *SmGGPPS*, *SmCPS*, *SmKSL*, and *SmTIIAS*. These selected genes cover key steps in the metabolic pathways, including upstream initiation, core condensation/cyclization, and downstream polymerization/modification steps, ensuring good representativeness and coverage. Additionally, we performed qRT-PCR analysis of five candidate TFs with significantly differential expression, including EVM0024997, EVM0002972, EVM0001404, EVM0020612, and EVM0023863. The qRT-PCR results showed high consistency with the expression trends observed in the transcriptomic data, confirming the robustness of the sequencing results. The expression patterns of these pathway genes are largely consistent with the accumulation patterns noted for salvianolic acids and tanshinones in this experimental system (Fig. 1).

4. Discussion

With the growing global demand for high-yield medicinal plants rich in bioactive compounds, the market continues to expand. Phytohormones have been widely used in plant metabolic engineering to significantly enhance both biomass production and the accumulation of bioactive compounds [10,45,46]. JA interacts with other phytohormones such as auxin, ethylene (ETH), GA, salicylic acid (SA), BR, and ABA, forming a complex signaling network. Through interconnected signaling pathways, these phytohormones collectively regulate plant growth, development, and the accumulation of metabolites [47]. The production of tanshinones and salvianolic acids, which are the major bioactive compounds present in *S. miltiorrhiza*, exhibits significant responsivity to various phytohormones. Exogenous application of ABA, MeJA, Indole-3-acetic acid (IAA), and GA, for instance, can promote the accumulation of tanshinones and salvianolic acids in *S. miltiorrhiza* by inducing the expression of *SPL6* [48]. This study utilized a hairy root culture system of *S. miltiorrhiza* combined with BR treatment at different time points, demonstrating that the contents of bioactive compounds such as tanshinones and salvianolic acids initially increased and then plateaued, with an overall enhancement in content. Collectively, these results indicate that BR treatment significantly promotes the accumulation of active components in *S. miltiorrhiza*, and to further clarify the underlying molecular mechanism, we performed transcriptome sequencing and in-depth analysis.

DEGs were identified in hairy roots following treatment with different concentrations of BR for different durations. Compared with the control group (0 h), the numbers of upregulated DEGs in the BR-1-1, BR-3-1, BR-1-5, and BR-3-5 groups were 3560, 3638, 2725, and 3060, respectively, with more upregulated genes having been detected following low-dose rather than high-dose BR treatment. Furthermore, under high-dose BR treatment, the inhibitory effect on gene expression became more pronounced as the duration of treatment grew longer. These findings indicate that BR treatment initiates a series of complex regulatory mechanisms in *S. miltiorrhiza*, upregulating the expression of genes encoding key enzymes and TFs involved in the salvianolic acid and tanshinone biosynthetic pathways, thereby promoting the accumulation of these bioactive components and enhancing the medicinal value of *S. miltiorrhiza*. The BR-mediated regulation of

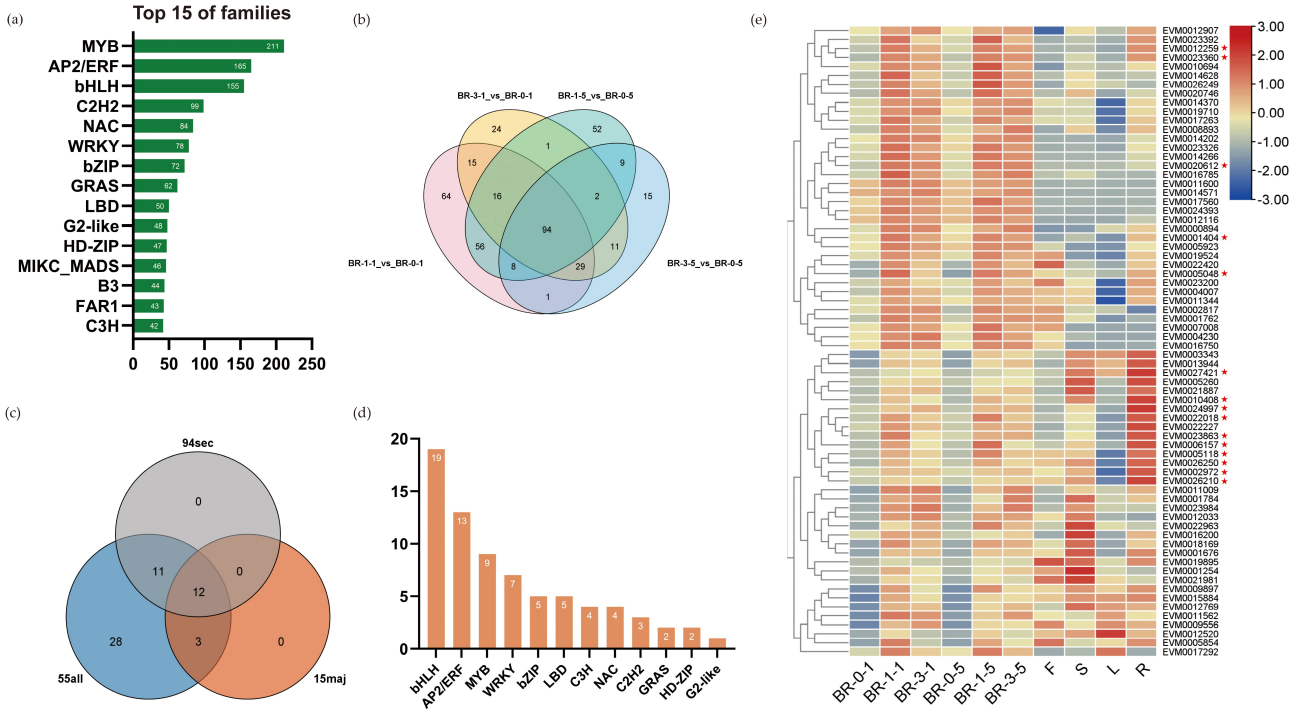

Fig. 5. Analysis annotated TFs among identified DEGs. (a) The top 15 TF families (15 maj) with >40 members. (b) Venn diagram of upregulated TFs among the four treatment groups, identifying a total of 94 commonly upregulated TFs (94 sec). (c) Venn diagram showing the relationships among the 55 TF families (55 all), 94 commonly upregulated TFs (94 sec), and the 15 major TF families (15 maj). (d) The 12 overlapping TF families for the 55 all, 94 sec, and 15 maj sets. (e) Expression profiles of 70 TFs under the four treatment conditions. Abbreviations: F, flower; S, stem; L, leaf; R, root, which denote the tissue expression profiles of TFs in *S. miltiorrhiza*. The heatmap was generated using $\log_2$-transformed FPKM values with row Z-score normalization. Red and blue respectively denote higher and lower expression levels. The star symbol indicates candidate transcription factors.

gene expression in *S. miltiorrhiza* hairy roots thus appears to exhibit distinct temporal dynamics and concentration specificity. Specifically, BR-induced transcriptional responses are rapidly activated within a short period, whereas the gene expression network gradually stabilizes with prolonged treatment; under high-dose BR treatment, transcriptional repression became more pronounced as the treatment duration increased. Furthermore, excessively high BR concentrations exert a discernible inhibitory effect on the upregulation of gene expression. Further examination of genes encoding key enzymes involved in tanshinone pathway (*e.g.*, *SmDXS*, *SmDXR*, *SmGGPPS*, *SmKSL)* and the salvianolic acid pathway (*e.g.*, *SmCYP98A*, *Sm4CL*, and *SmPAL*) revealed that most of these genes were initially upregulated in response to BR and then either slightly declined or remained elevated. These results further support the time- and concentration-dependent characteristics of BR-induced responses in *S. miltiorrhiza*.

TFs can directly regulate the expression of downstream genes by binding to specific cis-acting elements in the promoter regions of genes involved in the tanshinone and salvianolic acid biosynthetic pathways, thereby triggering the accumulation of these bioactive compounds in *S. miltiorrhiza*. To identify potential TFs involved in the regulation of the biosynthesis of these secondary metabolites following BR induction, we integrated HPLC data, expression patterns of genes encoding key enzymes in both pathways, and tissue-specific expression profiles of candidate TFs. A total of 15 candidate TFs were identified using this approach, including members of the bHLH, bZIP, AP2/ERF, MYB, NAC, C3H, C2H2, and WRKY families. Numerous studies have demonstrated that members of the bHLH, AP2/ERF, MYB, NAC, and WRKY families play crucial roles in regulating the accumulation of tanshinones and salvianolic acids in *S. miltiorrhiza* [10,44,49,50,51]. For instance, in *SmERF1L1*-overexpressing lines, key genes in the tanshinone biosynthetic pathway were consistently upregulated, with *SmDXR* showing the most significant increase in expression, which in turn led to the significant enhancement of tanshinone accumulation [52]. Overexpression of *SmMYB98* significantly enhanced the accumulation of both tanshinones and salvianolic acids in *S. miltiorrhiza*, whereas knockout lines showed a marked reduction in both compound classes [49]. In *SmbHLH3*-overexpression lines, phenolic acid biosynthetic genes (*e.g.*, *SmC4H1*, *SmTAT*, *SmHPPR*) and tanshinone biosynthetic genes (*e.g.*, *SmDXS3*, *SmKSL1*, *SmCPS1*) were significantly downregulated. Phenolic acid

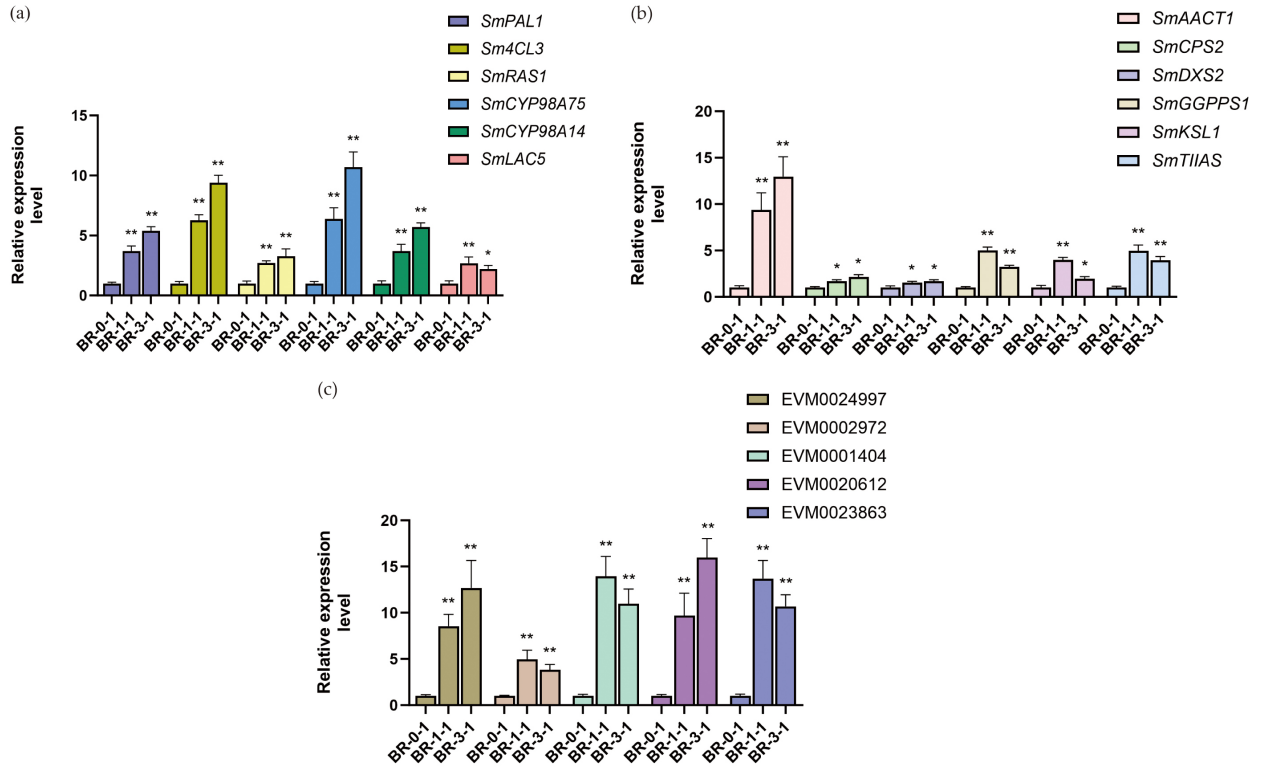

Fig. 6. qRT-PCR data of selected unigenes. (a) Expression levels of genes encoding key enzymes involved in the salvianolic acid biosynthetic pathway. (b) Expression levels of genes encoding key enzymes involved in the tanshinone biosynthetic pathway. (c) Expression levels of significantly differentially expressed candidate TFs identified by transcriptome analysis. All samples were treated with BR at 1 μM and collected at 0 h (BR-0-1), 1 h (BR-1-1), and 3 h (BR-3-1). Error bars indicate standard deviation (SD) (n = 5 biological replicates). Statistical significance was determined by Student's *t*-test. Asterisks denote statistically significant differences with BR-0-1: $*p < 0.05$; $**p < 0.01$.

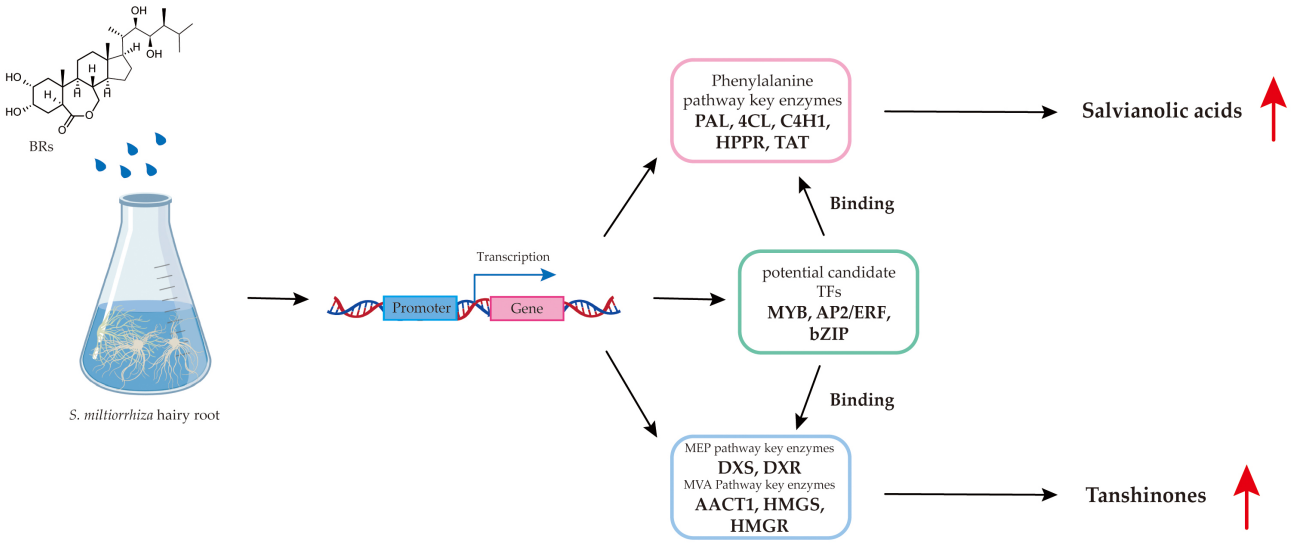

Fig. 7. Proposed regulatory mechanism of BR on tanshinone and salvianolic acid biosynthesis in *S. miltiorrhiza*. Created with BioGDP.com [56]. Red upward arrows indicate an increase in content.

content was decreased to 50% of the control level, whereas tanshinone content was even more profoundly affected, with CT and Tan IIA levels falling by 97% and 91%, respectively [50]. GO functional enrichment analysis indicated that most of these candidate TFs exhibit DNA-binding transcription factor activity and are implicated in chemical stim-

ulus responses. In addition to these TFs, the DEGs were functionally classified into three primary GO term clusters: catalytic activity (MF), membrane (CC), and metabolic and response processes (BP). BR drives and regulates the synthesis and transformation of secondary metabolites such as tanshinones and salvianolic acids by modulating the expression of genes encoding various functional enzymes [53]. Membranes serve as the primary localization sites of BR receptors (*e.g.*, BRI1), where BR signal perception and initial transduction predominantly occur, whereas altered expression of membrane-associated transporter genes can facilitate the transmembrane transport and distribution of secondary metabolites. As a plant hormone, BR can simultaneously activate secondary metabolic pathways and hormone signaling response pathways in *S. miltiorrhiza*, coordinating intracellular metabolic activities and responses to external signals through the regulation of gene expression networks.

To elucidate the major metabolic pathways associated with genes differentially expressed in response to BR treatment for different amounts of time, KEGG enrichment analysis was conducted. Salvianolic acids and tanshinones are derived from the phenylpropanoid and terpenoid pathways, respectively [54]. The enrichment analysis revealed significant enrichment in both the phenylpropanoid biosynthesis pathway and the terpenoid and polyketide metabolic pathways. The marked enrichment of these two pathways, coupled with the upregulation of key structural genes (*e.g.*, *SmPAL*, *SmC4H*, *Sm4CL*, *SmHMGR*, *SmKSL*), may constitute the primary reason for the accumulation of these bioactive metabolites. The coordinated upregulation of these two major secondary metabolic branches underscores the role that BR plays as a master regulator of secondary metabolism. Notably, the carbohydrate metabolism pathway exhibited the most significant enrichment. Given that the biosynthesis of both tanshinones and salvianolic acids is a highly energy-intensive process, and that their precursor molecules are directly derived from carbohydrate metabolism intermediates [15], these findings suggest that BR reprograms carbohydrate metabolism in *S. miltiorrhiza* to ensure sufficient energy and carbon skeleton availability for the biosynthesis of these bioactive compounds.

Following BR treatment, signal transduction takes place through the cell-surface receptor kinase BRI1, which heterodimerizes with the co-receptor BAK1, initiating a phosphorylation cascade. This cascade inhibits downstream negative regulator BIN2, leading to the subsequent dephosphorylation and nuclear translocation of the core TFs BES1 and BZR1. These signal transduction steps are highly conserved and well-characterized in plant species [26,55]. Based on this canonical pathway, we analyzed the expression dynamics of the core TFs SmBES1 and SmBZR1 following BR treatment. Our results showed that BR stimulation significantly induced the expression of both *SmBES1* and *SmBZR1* (**Supplementary Fig. 1**). Based on this observation, we propose the following regulatory network model: Once they have translocated into the nucleus, SmBES1/SmBZR1 may activate the secondary metabolic network through either or both of the following parallel or synergistic mechanisms: (1) directly binding to the promoter regions of genes encoding key enzymes involved in tanshinone and salvianolic acid biosynthesis (*e.g.*, *SmKSL*, *SmCYP98A*) to initiate their expression; or (2) binding to the promoter regions of candidate TFs identified in this study to activate their transcription, after which these secondary TFs further regulate the expression of metabolic pathway genes. Additionally, SmBES1/SmBZR1 may also physically interact with these candidate TFs to form transcriptional regulatory complexes, which then co-bind to the promoter regions of genes encoding downstream enzymes, thereby achieving synergistic regulation. Through this multi-layered regulatory network, BR ultimately promotes the efficient accumulation of bioactive compounds in *S. miltiorrhiza*.

This study may be subject to certain limitations. Firstly, only two BR concentrations (1 μM and 5 μM) were used, limiting our ability to precisely delineate effects associated with an optimal treatment concentration. Although the selected concentrations were based on preliminary experiments and evidence from the literature, future studies should employ a broader concentration gradient (*e.g.*, 0.1–20 μM) to systematically evaluate the dose-dependent effects of BR. Second, transcriptomic and metabolite analyses were restricted to short-term time points (0 h, 1 h, and 3 h) following BR treatment, limiting our understanding of the long-term regulatory effects of BR on secondary metabolism. Future studies should include extended time points (e.g., 6 h, 12 h, 24 h, or longer) to more comprehensively characterize the longitudinal regulatory effects of BR on secondary metabolism. In addition, although the transcriptomic data from this study were used to construct a potential regulatory network for BR-mediated secondary metabolism, the signal transduction mechanisms downstream of receptor recognition remain unclear. Future studies should therefore investigate the protein-DNA interactions (*e.g.*, via electrophoretic mobility shift assays and yeast two-hybrid assays) and protein-protein interactions (*e.g.*, via yeast two-hybrid and bimolecular fluorescence complementation) between key transcription factors and their target genes in the BR signaling pathway, thereby clarifying the downstream regulatory model and providing deeper insight into the molecular mechanisms by which BR regulates tanshinone and salvianolic acid biosynthesis. The continued pursuit of these research directions has the potential to further validate the proposed regulatory model, significantly strengthen the robustness and generalizability of the associated conclusions, and provide a more solid theoretical basis for the breeding of high-quality *S. miltiorrhiza* germplasm.

5. Conclusion

This study represents the first transcriptome-wide analysis aimed at establishing the effects of exogenous BR treatment on the regulation of major bioactive compounds in *S. miltiorrhiza*. Our findings reveal that BR promotes the accumulation of these metabolites by orchestrating the expression of key structural genes involved in both pathways, as well as the expression of the TFs that modulate these responses. Specifically, we demonstrated that BR treatment enhances the expression of pathway genes such as *SmC4H1*, *SmTAT*, *SmDXS*, and *SmKSL*. Furthermore, we identified 15 BR-responsive TFs and their potential regulatory networks, providing a valuable genetic resource for future metabolic engineering efforts (Fig. 7, Ref. [56]). Collectively, this study validates the use of BR as an effective elicitor to improve the quality of *S. miltiorrhiza* preparations.

Availability of Data and Materials

The datasets generated and analyzed during the current study are available from the corresponding author on reasonable request.

Author Contributions

Conceptualization, ZZ, QL and YH; methodology, ZZ and QL; software, QL, XS and WM; validation, WM, CH, RC, and YD; formal analysis, QL, ZZ, WM, and WW; investigation, ZZ, LY, WM and CH; resources, ZZ, QL and YH; data curation, WM; writing—original draft preparation, WM; writing—review and editing, ZZ and QL; visualization, WM and ZZ; supervision, ZZ; project administration, ZZ; funding acquisition, RC, LY and QL; All authors have read and agreed to the final version of the manuscript. All authors contributed to editorial changes in the manuscript. All authors have participated sufficiently in the work and agreed to be accountable for all aspects of the work.

Ethics Approval and Consent to Participate

Not applicable.

Acknowledgment

We are deeply grateful to the anonymous peer reviewers for their insightful comments and constructive suggestions, which have significantly enhanced the quality and presentation of this work.

Funding

This research was funded by the National Key Research and Development Program of China (Grant No. 2023YFC3504800), the Youth Program of National Natural Science Foundation of China (NSFC No. 82504959), the Natural Science Foundation of the Shanghai Science and Technology Commission (Project number: 24ZR1480900), and the National Natural Science Foundation of China (NSFC No. 32070327).

Conflicts of Interest

The authors declare no conflicts of interest.

Declaration of AI and AI-Assisted Technologies in the Writing Process

During the preparation of this work, the authors used DeepSeek-V3 and ChatGPT-4T to assist with literature searching, language refinement, and grammar checking. After using this tool, the authors thoroughly reviewed and edited the content as needed and take full responsibility for the integrity of the publication.

Supplementary Material

Supplementary material associated with this article can be found, in the online version, at https://doi.org/10.31083/FBL50834.

References

[1] Wei B, Sun C, Wan H, Shou Q, Han B, Sheng M, et al. Bioactive components and molecular mechanisms of Salvia miltiorrhiza Bunge in promoting blood circulation to remove blood stasis. Journal of Ethnopharmacology. 2023; 317: 116697. https://doi.org/10.1016/j.jep.2023.116697

[2] Shao S, Lv B, Wang M, Zeng S, Wang S, Yang Z, et al. Biosynthesis and regulatory mechanism of tanshinones and phenolic acids in Salvia miltiorrhiza. The Plant Journal : for Cell and Molecular Biology. 2025; 123: e70358. https://doi.org/10.1111/tpj.70358

[3] Jiang L, Li Y, Yu J, Wang J, Ju J, Dai J. A dry powder inhalable formulation of salvianolic acids for the treatment of pulmonary fibrosis: safety, lung deposition, and pharmacokinetic study. Drug Delivery and Translational Research. 2021; 11: 1958–1968. https://doi.org/10.1007/s13346-020-00857-7

[4] Yang L, Huang X, Wang Z, Guo Z, Ma C, Dong L, et al. Research progress on the pharmacological properties of active ingredients from Salvia miltiorrhiza: A review. Phytomedicine : International Journal of Phytotherapy and Phytopharmacology. 2025; 148: 157272. https://doi.org/10.1016/j.phymed.2025.157272

[5] Su CY, Ming QL, Rahman K, Han T, Qin LP. Salvia miltiorrhiza: Traditional medicinal uses, chemistry, and pharmacology. Chinese Journal of Natural Medicines. 2015; 13: 163–182. https://doi.org/10.1016/S1875-5364(15)30002-9

[6] Wang X, Yang Y, Liu X, Gao X. Pharmacological properties of tanshinones, the natural products from Salvia miltiorrhiza. Advances in Pharmacology (San Diego, Calif.). 2020; 87: 43–70. https://doi.org/10.1016/bs.apha.2019.10.001

[7] Abd Rashed A, Rathi DNG. Bioactive Components of *Salvia* and Their Potential Antidiabetic Properties: A Review. Molecules (Basel, Switzerland). 2021; 26: 3042. https://doi.org/10.3390/molecules26103042

[8] Begum G, Singh ND, Leishangthem GD, Banga HS. Amelioration of bleomycin induced pulmonary fibrosis by administration of Salvianolic acid B in mice. Veterinaria Italiana. 2022; 58: 87–101. https://doi.org/10.12834/VetIt.1703.9039.2

[9] Ren Y, Wang G, Su Y, Li J, Zhang H, Han J. Response of antioxidant activity, active constituent and rhizosphere microorganisms of Salvia miltiorrhiza to combined application of microbial inoculant, microalgae and biochar under Cu stress. The

Science of the Total Environment. 2024; 925: 171812. https://doi.org/10.1016/j.scitotenv.2024.171812
[10] Zheng H, Fu X, Shao J, Tang Y, Yu M, Li L, et al. Transcriptional regulatory network of high-value active ingredients in medicinal plants. Trends in Plant Science. 2023; 28: 429–446. https://doi.org/10.1016/j.tplants.2022.12.007
[11] Wang H, Wang A, Pu H, Yang Y, Ling Z, Xu H, et al. Induction, Flavonoids Contents, and Bioactivities Analysis of Hairy Roots and True Roots of *Tetrastigma hemsleyanum* Diels et Gilg. Molecules (Basel, Switzerland). 2023; 28: 2686. https://doi.org/10.3390/molecules28062686
[12] Alcalde MA, Perez-Matas E, Escrich A, Cusido RM, Palazon J, Bonfill M. Biotic Elicitors in Adventitious and Hairy Root Cultures: A Review from 2010 to 2022. Molecules (Basel, Switzerland). 2022; 27: 5253. https://doi.org/10.3390/molecules27165253
[13] Reshi ZA, Ahmad W, Lukatkin AS, Javed SB. From Nature to Lab: A Review of Secondary Metabolite Biosynthetic Pathways, Environmental Influences, and In Vitro Approaches. Metabolites. 2023; 13: 895. https://doi.org/10.3390/metabo13080895
[14] Cao R, Lv B, Shao S, Zhao Y, Yang M, Zuo A, et al. The SmMYC2-SmMYB36 complex is involved in methyl jasmonate-mediated tanshinones biosynthesis in Salvia miltiorrhiza. The Plant Journal : for Cell and Molecular Biology. 2024; 119: 746–761. https://doi.org/10.1111/tpj.16793
[15] Li L, Wang D, Zhou L, Yu X, Yan X, Zhang Q, et al. JA-Responsive Transcription Factor SmMYB97 Promotes Phenolic Acid and Tanshinone Accumulation in *Salvia miltiorrhiza*. Journal of Agricultural and Food Chemistry. 2020; 68: 14850–14862. https://doi.org/10.1021/acs.jafc.0c05902
[16] Deng C, Wang Y, Huang F, Lu S, Zhao L, Ma X, et al. SmMYB2 promotes salvianolic acid biosynthesis in the medicinal herb Salvia miltiorrhiza. Journal of Integrative Plant Biology. 2020; 62: 1688–1702. https://doi.org/10.1111/jipb.12943
[17] Chen M, Xiao Y, Tan R, Zheng X, Lv Z, Zhao S. The APETALA2/ETHYLENE RESPONSE FACTOR transcription factor SmERF005 negatively regulates meristem cell division and biosynthesis of phenolic acids and diterpenoids in Salvia miltiorrhiza hairy roots. International Journal of Biological Macromolecules. 2025; 311: 143688. https://doi.org/10.1016/j.ijbiomac.2025.143688
[18] Liu T, Shi M, Yang Y, Zhu R, Wang Y, Li L, et al. SmbZIP5 Integrates Abscisic and Jasmonic Acid Signalling to Positively Regulate Tanshinone Biosynthesis in Salvia miltiorrhiza. Plant Biotechnology Journal. 2025; 23: 5817–5832. https://doi.org/10.1111/pbi.70344
[19] He P, Zhu L, Zhou X, Fu X, Zhang Y, Zhao P, et al. Gibberellic acid promotes single-celled fiber elongation through the activation of two signaling cascades in cotton. Developmental Cell. 2024; 59: 723–739.e4. https://doi.org/10.1016/j.devcel.2024.01.018
[20] Yu H, Yao R, Zhang S, Chen Y, Liang C, Liu Y, et al. bHLH130 mediates gibberellin signaling to regulate tanshinone biosynthesis in *Salvia miltiorrhiza*. Acta Pharmaceutica Sinica. B. 2026; 16: 1747–1761. https://doi.org/10.1016/j.apsb.2025.11.041
[21] Li W, Xing B, Mao R, Bai Z, Yang D, Xu J, et al. SmGRAS3 negatively responds to GA signaling while promotes tanshinones biosynthesis in Salvia miltiorrhiza. Industrial Crops and Products. 2020; 144: 112004.
[22] Kaur Kohli S, Bhardwaj A, Bhardwaj V, Sharma A, Kalia N, Landi M, et al. Therapeutic Potential of Brassinosteroids in Biomedical and Clinical Research. Biomolecules. 2020; 10: 572. https://doi.org/10.3390/biom10040572
[23] Wei Z, Li J. Regulation of Brassinosteroid Homeostasis in Higher Plants. Frontiers in Plant Science. 2020; 11: 583622. https://doi.org/10.3389/fpls.2020.583622
[24] Oh MH, Honey SH, Tax FE. The Control of Cell Expansion, Cell Division, and Vascular Development by Brassinosteroids: A Historical Perspective. International Journal of Molecular Sciences. 2020; 21: 1743. https://doi.org/10.3390/ijms21051743
[25] Massolo JF, Díaz AA. Brassinosteroid biology, potential uses in post-harvest technology and future challenges. Postharvest Biology and Technology. 2024; 212: 112853.
[26] Gampala SS, Kim TW, He JX, Tang W, Deng Z, Bai MY, et al. An essential role for 14-3-3 proteins in brassinosteroid signal transduction in Arabidopsis. Developmental Cell. 2007; 13: 177–189. https://doi.org/10.1016/j.devcel.2007.06.009
[27] Fanai S, Bakhshi D, Abbaszadeh B. Physiological and biochemical characteristics of milk thistle (*Silybum marianum* (L.) Gaertn) as affected by some plant growth regulators. Food Science & Nutrition. 2024; 12: 6022–6033. https://doi.org/10.1002/fsn3.4233
[28] Ahanger MA, Mir RA, Alyemeni MN, Ahmad P. Combined effects of brassinosteroid and kinetin mitigates salinity stress in tomato through the modulation of antioxidant and osmolyte metabolism. Plant Physiology and Biochemistry : PPB. 2020; 147: 31–42. https://doi.org/10.1016/j.plaphy.2019.12.007
[29] Miao R, Li C, Liu Z, Zhou X, Chen S, Zhang D, et al. The Role of Endogenous Brassinosteroids in the Mechanisms Regulating Plant Reactions to Various Abiotic Stresses. Agronomy. 2024; 14: 356–374.
[30] Manghwar H, Hussain A, Ali Q, Liu F. Brassinosteroids (BRs) Role in Plant Development and Coping with Different Stresses. International Journal of Molecular Sciences. 2022; 23: 1012. https://doi.org/10.3390/ijms23031012
[31] Qiu R, Zhou Y, Mao J. Brassinosteroid Signaling Dynamics: Ubiquitination-Dependent Regulation of Core Signaling Components. International Journal of Molecular Sciences. 2025; 26: 4502. https://doi.org/10.3390/ijms26104502
[32] Nikolić B, Jovanović V, Knežević B, Nikolić Z, Babović-Đorđević M. Mode of Action of Brassinosteroids: Seed Germination and Seedling Growth and Development-One Hypothesis. International Journal of Molecular Sciences. 2025; 26: 2559. https://doi.org/10.3390/ijms26062559
[33] Hussain S, Nanda S, Ashraf M, Siddiqui AR, Masood S, Khaskheli MA, et al. Interplay Impact of Exogenous Application of Abscisic Acid (ABA) and Brassinosteroids (BRs) in Rice Growth, Physiology, and Resistance under Sodium Chloride Stress. Life (Basel, Switzerland). 2023; 13: 498. https://doi.org/10.3390/life13020498
[34] Zhou YL, You XY, Wang XY, Cui LH, Jiang ZH, Zhang KP. Exogenous 24-Epibrassinolide Enhanced Drought Tolerance and Promoted BRASSINOSTEROID-INSENSITIVE2 Expression of Quinoa. Plants (Basel, Switzerland). 2024; 13: 873. https://doi.org/10.3390/plants13060873
[35] Wang H, Asker K, Zhan C, Wang N. Transcriptomic and Metabolic Analysis of Fruit Development and Identification of Genes Involved in Raffinose and Hydrolysable Tannin Biosynthesis in Walnuts. Journal of Agricultural and Food Chemistry. 2021; 69: 8050–8062. https://doi.org/10.1021/acs.jafc.1c02434
[36] Li Ym, Wang Xr, Yang G, Yan Tt, Hu Xc, Peng L, et al. Profiling the accumulation of ten bioactive compounds in Rheum officinale across different growth years using integrated HPLC and transcriptomic approaches. Medicinal Plant Biology. 2025; 4: e022.
[37] Kim D, Langmead B, Salzberg SL. HISAT: a fast spliced aligner with low memory requirements. Nature Methods. 2015; 12: 357–360. https://doi.org/10.1038/nmeth.3317
[38] Anders S, Pyl PT, Huber W. HTSeq–a Python framework to work with high-throughput sequencing data. Bioinformatics (Oxford, England). 2015; 31: 166–169. https://doi.org/10.1093/

bioinformatics/btu638
[39] Leng N, Dawson JA, Thomson JA, Ruotti V, Rissman AI, Smits BMG, et al. EBSeq: an empirical Bayes hierarchical model for inference in RNA-seq experiments. Bioinformatics (Oxford, England). 2013; 29: 1035–1043. https://doi.org/10.1093/bioinformatics/btt087
[40] Benjamini Y, Drai D, Elmer G, Kafkafi N, Golani I. Controlling the false discovery rate in behavior genetics research. Behavioural Brain Research. 2001; 125: 279–284. https://doi.org/10.1016/s0166-4328(01)00297-2
[41] Ashburner M, Ball CA, Blake JA, Botstein D, Butler H, Cherry JM, et al. Gene ontology: tool for the unification of biology. The Gene Ontology Consortium. Nature Genetics. 2000; 25: 25–29. https://doi.org/10.1038/75556
[42] Draghici S, Khatri P, Tarca AL, Amin K, Done A, Voichita C, et al. A systems biology approach for pathway level analysis. Genome Research. 2007; 17: 1537–1545. https://doi.org/10.1101/gr.6202607
[43] Xing B, Liang L, Liu L, Hou Z, Yang D, Yan K, et al. Overexpression of SmbHLH148 induced biosynthesis of tanshinones as well as phenolic acids in Salvia miltiorrhiza hairy roots. Plant Cell Reports. 2018; 37: 1681–1692. https://doi.org/10.1007/s00299-018-2339-9
[44] Chen Y, Wang Y, Guo J, Yang J, Zhang X, Wang Z, et al. Integrated Transcriptomics and Proteomics to Reveal Regulation Mechanism and Evolution of *SmWRKY61* on Tanshinone Biosynthesis in *Salvia miltiorrhiza* and *Salvia castanea*. Frontiers in Plant Science. 2022; 12: 820582. https://doi.org/10.3389/fpls.2021.820582
[45] Li H, Jiang X, Mashiguchi K, Yamaguchi S, Lu S. Biosynthesis and signal transduction of plant growth regulators and their effects on bioactive compound production in Salvia miltiorrhiza (Danshen). Chinese Medicine. 2024; 19: 102. https://doi.org/10.1186/s13020-024-00971-5
[46] Lu S. Biosynthesis and Regulatory Mechanisms of Bioactive Compounds in Salvia miltiorrhiza, a Model System for Medicinal Plant Biology. Critical Reviews in Plant Sciences. 2021; 40: 243–283.
[47] Wang Y, Mostafa S, Zeng W, Jin B. Function and Mechanism of Jasmonic Acid in Plant Responses to Abiotic and Biotic Stresses. International Journal of Molecular Sciences. 2021; 22: 8568. https://doi.org/10.3390/ijms22168568
[48] Cao Y, Chen R, Wang WT, Wang DH, Cao XY. SmSPL6 Induces Phenolic Acid Biosynthesis and Affects Root Development in *Salvia miltiorrhiza*. International Journal of Molecular Sciences. 2021; 22: 7895. https://doi.org/10.3390/ijms22157895
[49] Hao X, Pu Z, Cao G, You D, Zhou Y, Deng C, et al. Tanshinone and salvianolic acid biosynthesis are regulated by *SmMYB98* in *Salvia miltiorrhiza* hairy roots. Journal of Advanced Research. 2020; 23: 1–12. https://doi.org/10.1016/j.jare.2020.01.012
[50] Zhang C, Xing B, Yang D, Ren M, Guo H, Yang S, et al. SmbHLH3 acts as a transcription repressor for both phenolic acids and tanshinone biosynthesis in Salvia miltiorrhiza hairy roots. Phytochemistry. 2020; 169: 112183. https://doi.org/10.1016/j.phytochem.2019.112183
[51] Zhang Y, Ji A, Xu Z, Luo H, Song J. The AP2/ERF transcription factor SmERF128 positively regulates diterpenoid biosynthesis in Salvia miltiorrhiza. Plant Molecular Biology. 2019; 100: 83–93. https://doi.org/10.1007/s11103-019-00845-7
[52] Huang Q, Sun M, Yuan T, Wang Y, Shi M, Lu S, et al. The AP2/ERF transcription factor SmERF1L1 regulates the biosynthesis of tanshinones and phenolic acids in Salvia miltiorrhiza. Food Chemistry. 2019; 274: 368–375. https://doi.org/10.1016/j.foodchem.2018.08.119
[53] Xu Y, Geng L, Zhao S. Biosynthesis of bioactive ingredients of Salvia miltiorrhiza and advanced biotechnologies for their production. Biotechnology & Biotechnological Equipment. 2018; 32: 1367–1377.
[54] Cheng Y, Hong X, Zhang L, Yang W, Zeng Y, Hou Z, et al. Transcriptomic analysis provides insight into the regulation mechanism of silver ions (Ag+) and jasmonic acid methyl ester (MeJA) on secondary metabolism in the hairy roots of Salvia miltiorrhiza Bunge (Lamiaceae). Medicinal Plant Biology. 2023; 2: 3–13.
[55] Li QF, Lu J, Yu JW, Zhang CQ, He JX, Liu QQ. The brassinosteroid-regulated transcription factors BZR1/BES1 function as a coordinator in multisignal-regulated plant growth. Biochimica et Biophysica Acta. Gene Regulatory Mechanisms. 2018; 1861: 561–571. https://doi.org/10.1016/j.bbagrm.2018.04.003
[56] Jiang S, Li H, Zhang L, Mu W, Zhang Y, Chen T, et al. Generic Diagramming Platform (GDP): a comprehensive database of high-quality biomedical graphics. Nucleic Acids Research. 2025; 53: D1670–D1676. https://doi.org/10.1093/nar/gkae973